Unveiling the mid-plane temperature and mass distribution in the giant-planet formation zone

Ke Zhang[1]**, Edwin A. Bergin**[1]**, Geoffrey A. Blake**[2]**,**
L. Ilsedore Cleeves[3] **and Kamber R. Schwarz**[1]

[1]Department of Astronomy, University of Michigan, 311 West Hall,
1085 S University Ave., Ann Arbor, MI 48109, USA
email: `kezhang@umich.edu`

[2]Division of Geological & Planetary Sciences, California Institute of Technology,
MC 150-21, Pasadena, CA 91125, USA

[3]Harvard-Smithsonian Center for Astrophysics, 60 Garden Street, Cambridge, MA 02138, USA

Abstract. Core-accretion theory predicts that the formation of giant planets predominantly occurs at the dense mid-plane of the inner $\sim$50 AU of protoplanetary disks. However, due to observational limitation, this critical region remains to be the least charted area in protoplanetary disks. With its great sensitivity, ALMA recently started to image optically thin line emissions arisen from the mid-plane of the inner 50AU in nearby disks, which unlocks an exciting new path to directly constrain the physical properties of the giant planet formation zone through gas tracers. Here we present the first spatially resolved observations of the $^{13}C^{18}O$ J=3-2 line emission in the TW Hya disk. We show that this emission is optically thin even inside the CO mid-plane snowline. Combining it with the $C^{18}O$ J=3-2 images and the previously detected HD J=1-0 flux, we directly constrain the mid-plane temperature and optical depths of the CO gas and dust. We report a mid-plane CO snowline at 20.5 ± 1.3 AU, a mid-plane temperature distribution of $27_{-3}^{+4} \times (R/20.5 \mathrm{AU})^{-0.47_{-0.07}^{+0.06}}$ K, and a gas mass distribution of $13_{-5}^{+8} \times (R/20.5 \mathrm{AU})^{-0.9_{-0.3}^{+0.4}}$ g cm^{-2} between 5-20.5 AU in the TW Hya protoplanetary disk. We find a total gas/mm-sized dust mass ratio of 140 ± 40 in this region, suggesting that $\sim$2.4 earth mass of dust aggregates have grown to > cm sizes (and perhaps much larger).

Keywords. planet formation, protoplanetary disks, astrochemistry

1. Introduction

Protoplanetary disks set the stage for planet formation. In particular, the equatorial plane of a disk, the so-called *mid-plane,* is the dominant location where planet formation occurs. The mid-plane region is the densest place along the vertical direction of a disk and it is the bulk mass reservoir for dust growth, drift, planetesimal formation, and ultimately the birth site of a planetary system. As a result, the basic properties of the mid-plane, such as temperature and density, are crucial initial inputs for planet formation models (Pollack *et al.* 1996; Benz *et al.* 2014).

However, even the most basic properties of the mid-plane is largely unconstrained. The most commonly used constraints of the surface mass distribution and the mid-plane temperature structure are based on spatially resolved observations of (sub)mm continuum emission of dust grains. At these wavelengths, the dust continuum emission is expected to be mostly optically thin. If the dust opacity and gas-to-dust mass ratio are constant throughout the disk, the mass distribution and temperature structure can be self-consistently constrained from spatially resolved images of dust continuum emission

(e.g. Andrews & Williams 2007; Isella *et al.* 2009). However, the key assumption of constant gas-to-dust mass ratio and dust opacity is highly problematic. Growing observations show that the gas and millimeter-sized dust grains may have distinctive spatial distributions (Andrews *et al.* 2012; Rosenfeld *et al.* 2013b; Zhang *et al.* 2014), and the dust opacities vary significantly with radius in a disk (Pérez *et al.* 2012; ALMA Partnership *et al.* 2015).

Due to these large uncertainty in dust properties, an independent gas tracer is necessary to measure the mass distributions and temperature structures at the mid-plane of protoplanetary disks. But the dominant gas constituent H_2 lacks emissivity at the low temperatures present throughout most regions of the disk and thus cannot be directly measured. Instead, CO is typically used as a tracer of gaseous materials (Piétu *et al.* 2007; Ansdell *et al.* 2016). It has the advantages of being chemically stable in the absence of ionizing radiation and being resistant to freeze-out at the mid-plane out to a large radius (Qi *et al.* 2013).

The radius that CO starts to freeze-out at the mid-plane is called the mid-plane CO snowline. It sets an important boundary – outside the snowline, the CO gas condenses at different vertical heights and thus its lines provide no constraints on physical conditions at the mid-plane (Rosenfeld *et al.* 2013a). Inside the snowline, however, CO vapor has nearly constant abundance in both the radial and vertical directions (except for the very surface layer, where CO is photo-dissociated, but the surface layer only contains a negligible fraction of the total gas column density).

Using CO as a global tracer of mass distribution usually face two problems. First of all, the most abundant CO isotopologues ^{12}CO and ^{13}CO readily become optically thick near the disk surface (Beckwith & Sargent 1993; Piétu *et al.* 2007) and thus their line intensities cannot constrain the bulk mass reservoir at the mid-plane. Moreover, beyond the CO mid-plane snowline, CO gas freezes onto grains at different heights in the disk atmosphere (Schwarz *et al.* 2016). Thus the derived gas structure and, crucially, the radial surface density, is highly model dependent (Flaherty *et al.* 2015; Williams & McPartland 2016).

Here we aim to directly probe the mid-plane region inside the CO mid-plane snowline with an optically thin CO line. We targeted the $^{13}C^{18}O$ and $C^{18}O$ J=3-2 transitions (on average 38433 and 577 times less abundant than $^{12}C^{16}O$ in the interstellar medium, respectively) in the TW Hya protoplanetary disks. It is one of the nearest disks ($\sim$55 pc, van Leeuwen 2007), and also is one of the best-studied disk systems. This disk makes a useful analog to the solar nebula: the central star has a stellar mass about 0.6-0.8 $M_\odot$ (Webb *et al.* 1999); the disk itself has a total mass (gas and dust) of $\sim$0.05 $M_\odot$ (Bergin *et al.* 2013). This is comparable to the total mass of 0.01 $M_\odot$ in the Minimum Mass Solar Nebula (MMSN) which is the lowest possible mass needed to reproduce the Solar System (Hayashi 1981). The age of TW Hya is 8 ± 4 Myr (Donaldson *et al.* 2016), within the expected window for giant planet formation (Chabrier *et al.* 2014).

2. Observations

The observations of the TW Hya protoplanetary disk were carried out with the Atacama Large Millimeter/submillimeter Array (ALMA) on 2015 March 8 (Cycle 3 project #2015.1.00308.S, P.I. Bergin). The lengths of baselines were between 15-460 m (16-492 kλ) and the total on-source integration time was 67.5 min. Three SPWs were used for line observations with a resolution of $\delta\nu = 122$ kHz (a spectral resolution of 0.23 km s^{-1} after the default Hanning smoothing is applied), and the fourth one was dedicated for continuum observations with a total bandwidth of 1.875 GHz.
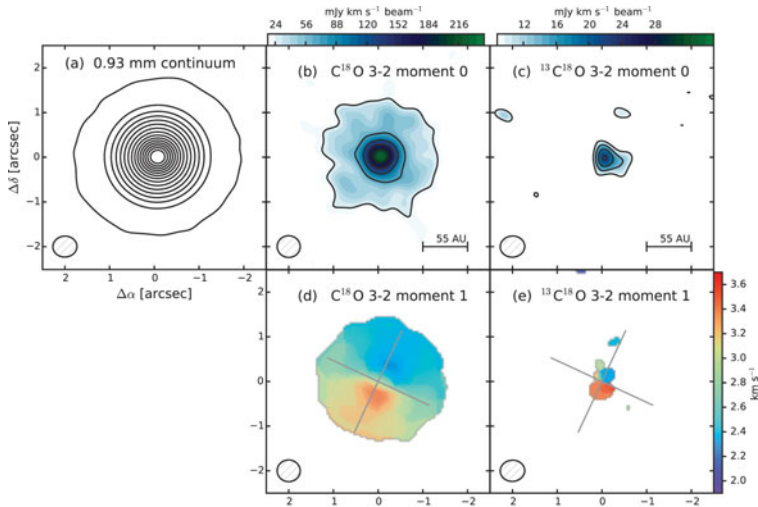
Figure 1. ALMA observations of the $C^{18}O$ and $^{13}C^{18}O$ (3-2) line emission in the TW Hya protoplanetary disk. (a) Dust continuum emission at 0.93 mm. The contours linearly span 10 to 3100σ. (b-c) Integrated emission from the $C^{18}O$ and $^{13}C^{18}O$ J=3-2 transitions. The $C^{18}O$ contour levels start at 3σ and increase in 5σ steps; the $^{13}C^{18}O$ contour levels are $[2,4,5,6]\sigma$. (d-e) Intensity weighted velocity maps of $C^{18}O$ and $^{13}C^{18}O$, showing that the emissions arise from a disk in Keplerian rotation.

The visibility data were calibrated by ALMA staff following standard procedures. We further performed self-calibration on the calibrated data in phase and amplitude in CASA 4.6.12, using the dedicated continuum observations. The self-calibrated phase and gain solutions were then applied to the three line SPWs. The data were subsequently continuum subtracted using line free channels. We generated synthesized images using a CLEAN deconvolution with a manual mask (Briggs weighting with a robust parameter of 0.5). For the 321 GHz continuum emission map, the synthesized beam is $0.54'' \times 0.47''$ (position angle = -87 degrees). The noise level of the $C^{18}O$ line images is 6.5 mJy beam^{-1} in each 0.23 km s^{-1} wide velocity bin, and 4 mJy beam^{-1} in the $^{13}C^{18}O$ line image cube.

Both $C^{18}O$ and $^{13}C^{18}O$ J=3-2 line emissions were robustly detected in the TW Hya disk, with a peak-to-noise ratio of 29 and 5, respectively. The synthesized images of line and continuum emission are displayed in Figure 1. Both line emissions show a bright central peak, and $C^{18}O$ line also shows broad diffuse emission in the outer disk. This morphology is consistent with the theoretical expectation that the mid-plane temperature gradually decreases with radius and that beyond the mid-plane CO snowline most of the CO condenses into ice. The central peaks of the $^{13}C^{18}O$ and $C^{18}O$ emission are 15-40% larger than the $0.5''$ ($\sim$27.5 AU) synthesized beam, suggesting that the region inside the CO snowline is partially resolved. In practice, the data provide constraints on smaller spatial scales than the synthesized beam, since it is also spectrally resolved (0.23 km s^{-1} resolution) and the velocity field is known to be Keplerian (see Figure 1 (d-e)). Inside the central bright peak emission, the peak flux of the $C^{18}O$ line emission is only 8 times stronger than the $^{13}C^{18}O$ emission, significantly less than the average isotopic ratio of $^{12}C/^{13}C = 69$ in the ISM. Therefore, the $C^{18}O$ line emission is optically thick inside the mid-plane CO snowline.

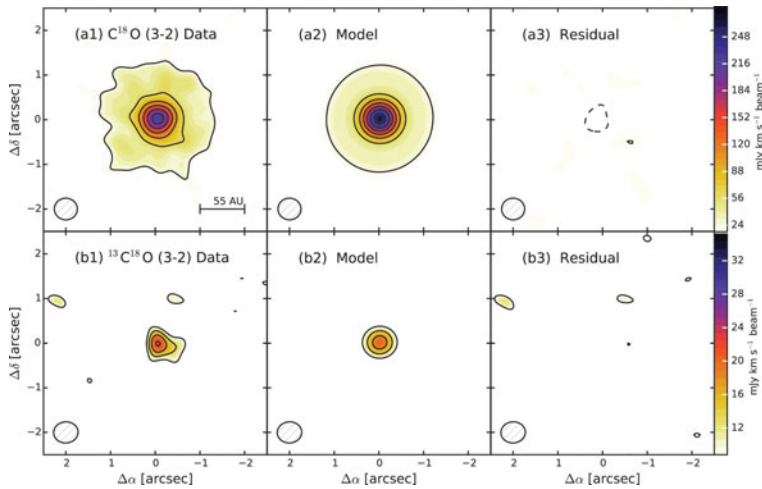**Figure 2.** Comparisons of the $C^{18}O$ and $^{13}C^{18}O$ J=3-2 emission from the TW Hya disk with the best fitting model. The contour levels are the same as Figure 1(b-c).

3. Modeling

To retrieve the physical properties in the mid-plane, we use a parameterized disk model to reproduce the observations. Readers can find a full description of the model and the Markov chain Monte Carlo fitting algorithm in Zhang *et al.* (2017) and we briefly describe key elements of the modeling here.

We assume that the $^{13}C^{18}O$ and $C^{18}O$ emission arises predominately from the mid-plane or immediately adjacent regions. As the vertical temperature structures in proto-planetary disks are expected to be nearly isothermal within one scale height (Dullemond & Dominik 2004), both line emission can be characterized by the mid-plane temperature that is only a function of radius. This assumption is reasonable since $C^{18}O$ and $^{13}C^{18}O$ are 10^{-10}–10^{-6} times less abundant than H_2 (Wilson 1999).

To include continuum extinction from dust, we model the $C^{18}O$, $^{13}C^{18}O$ line emission and dust continuum simultaneously. For the dust emission, we use the radial profile of 345 GHz continuum emission of TW Hya derived from 1 AU resolution ALMA long baseline observations (Andrews *et al.* 2016). The advantage of using such high-resolution continuum emission is that we do not need to assume a function for the radial distribution of continuum optical depth. For the line emission, we use simple power-law functions to characterize the radial profiles of the temperature and integrated line strength. The best-fitting model is plotted in Figure 2 in comparison with the data.

4. Results

We report the first direct measurement of the mid-plane CO snowline at 20.5 ± 1.3 AU and a mid-plane temperature distribution of $27^{+4}_{-3} \times (R/20.5 \text{AU})^{-0.47^{+0.06}_{-0.07}}$ K in the TW Hya disk. We find that the $^{13}C^{18}O$ J=3-2 emission is optically thin ($\tau < 0.2$) throughout the disk and the dust continuum emission is moderately optically thin ($\tau \sim 0.5$) inside the CO mid-plane snowline. The two optical depths suggest that the $^{13}C^{18}O$ line emission arises from both sides of the disk and thus provides model-independent constraints on the gas mass distribution. Inside the mid-plane CO snowline, the $C^{18}O$ emission is optically thick ($\tau \sim 8$) and thus provides direct constraints on the gas temperature instead

of the mass distribution. Outside the mid-plane CO snowline, the $C^{18}O$ emission is optically thin. The observations provide constraints on physical properties of the mid-plane between 5-20.5 AU of the TW Hya disk: the outer limit is the mid-plane CO snowline location (beyond that CO condenses at the mid-plane); the inner boundary is limited by the radius of 10% cumulative flux at the highest velocity channel with a $^{13}C^{18}O$ emission detection.

With the temperature and optical depths from the best-fitting model, we can derive the column density distribution of $^{13}C^{18}O$ and then the gas mass distribution for a given $^{13}C^{18}O$ abundance ($x_{^{13}C^{18}O}$). Here we employ the spatially unresolved HD J=1-0 line flux of the TW Hya disk to estimate the $x_{^{13}C^{18}O}$ (Bergin *et al.* 2013). Combining the uncertainties in our model parameters and in the HD line flux, we find $x_{^{13}C^{18}O} = 1.7^{+1.3}_{-0.8} \times 10^{-10}$ and $\Sigma_{gas} = 13^{+8}_{-5} \times (R/20.5\,AU)^{-0.87^{+0.38}_{-0.26}}$ g cm^{-2} between 5-20.5 AU (for details, see Zhang *et al.* 2017).

Another constraint from our modeling is the optical depth of dust continuum emission at 0.93 mm between 5-20.5 AU. The optical depth is a combined result of dust mass and opacity. Recent observations have shown that the dust opacity may vary significantly with radius and as a result it is very challenging to measure the surface density profile of the dust mass. Due to these uncertainties, here we only derive a total gas-to-mass ratio for the region inside the CO mid-plane snowline. We adopt a constant dust opacity $\kappa(0.93\,\text{mm})$ = 3.1 cm^{2}g^{-1}, a value similar to previous studies for the TW Hya disk (Andrews *et al.* 2012; Hogerheijde *et al.* 2016).

We measure the total gas-to-mm-sized dust ratio is 140^{+43}_{-31} for the 5-20.5 AU region, much higher than the typical ratio of 100 in molecular clouds. In order to recover a gas-to-dust ratio of 100, we find that $2.4^{+3.2}_{-2.0}$ $M_\oplus$ solid masses are missing. This estimation is actually a lower limit, because the dust radial drift to the inner region should in general decrease the total gas-to-dust ratio in the inner disk (Birnstiel *et al.* 2012) and because the overall gas surface density also decreases with time. Therefore more than $2.4\,M_\oplus$ masses of solids may have grown to at least centimeter-sized and perhaps much larger bodies in the TW Hya disk.

Our observations demonstrate the possibility to use optically thin CO isotopologue lines to probe physical properties at the mid-plane of nearby protoplanetary disks. In the next a few years, ALMA will be able to carry out similar observations for more disks and provide critical constraints on the conditions of planet formation sites.

References

ALMA Partnership, Brogan, C. L., Pérez, L. M., *et al.* 2015, ApJL, 808, L3

Andrews, S. M. & Williams, J. P. 2007, ApJ, 671, 1800

Andrews, S. M., Wilner, D. J., Hughes, A. M., *et al.* 2012, ApJ, 744, 162

Andrews, S. M., Wilner, D. J., Zhu, Z., *et al.* 2016, ApJL, 820, L40

Ansdell, M., Williams, J. P., van der Marel, N., *et al.* 2016, ApJ, 828, 46

Beckwith, S. V. W. & Sargent, A. I. 1993, ApJ, 402, 280

Benz, W., Ida, S., Alibert, Y., Lin, D., & Mordasini, C. 2014, Protostars and Planets VI, 691

Bergin, E. A., Cleeves, L. I., Gorti, U., *et al.* 2013, Nature , 493, 644

Birnstiel, T., Klahr, H., & Ercolano, B. 2012, A&A, 539, A148

Chabrier, G., Johansen, A., Janson, M., & Rafikov, R. 2014, Protostars and Planets VI, 619

Donaldson, J. K., Weinberger, A. J., Gagné, J., *et al.* 2016, ApJ, 833, 95

Dullemond, C. P. & Dominik, C. 2004, A&A, 417, 159

Flaherty, K. M., Hughes, A. M., Rosenfeld, K. A., *et al.* 2015, ApJ, 813, 99

Hayashi, C. 1981, PTPS, 70, 35

Hogerheijde, M. R., Bekkers, D., Pinilla, P., *et al.* 2016, A&A, 586, A99

Isella, A., Carpenter, J. M., & Sargent, A. I. 2009, ApJ, 701, 260

Pérez, L. M., Carpenter, J. M., Chandler, C. J., *et al.* 2012, ApJL, 760, L17

Piétu, V., Dutrey, A., & Guilloteau, S. 2007, A&A, 467, 163

Pollack, J. B., Hubickyj, O., Bodenheimer, P., *et al.* 1996, *Icarus*, 124, 62

Qi, C., Öberg, K. I., Wilner, D. J., *et al.* 2013, *Science*, 341, 630

Rosenfeld, K. A., Andrews, S. M., Hughes, A. M., Wilner, D. J., & Qi, C. 2013a, ApJ, 774, 16

Rosenfeld, K. A., Andrews, S. M., Wilner, D. J., Kastner, J. H., & McClure, M. K. 2013b, ApJ, 775, 136

Schwarz, K. R., Bergin, E. A., Cleeves, L. I., *et al.* 2016, ApJ, 823, 91

van Leeuwen, F. 2007, A&A, 474, 653

Webb, R. A., Zuckerman, B., Platais, I., *et al.* 1999, ApJL, 512, L63

Williams, J. P. & McPartland, C. 2016, ApJ, 830, 32

Wilson, T. L. 1999, *Reports on Progress in Physics*, 62, 143

Zhang, K., Bergin, E. A., Blake, G. A., Cleeves, L. I., & Schwarz, K. R. 2017, Nature Astronomy, 1, 0130

Zhang, K., Isella, A., Carpenter, J. M., & Blake, G. A. 2014, ApJ, 791, 42